Stratiform Rain in the Tropics as Seen by the TRMM Precipitation Radar*

COURTNEY SCHUMACHER AND ROBERT A. HOUZE JR.

Department of Atmospheric Sciences, University of Washington, Seattle, Washington

(Manuscript received 6 September 2002, in final form 9 December 2002)

ABSTRACT

Across the Tropics (20°N–20°S), the Tropical Rainfall Measuring Mission (TRMM) Precipitation Radar (PR) indicates that for reflectivities ≥17 dB*Z*, stratiform precipitation accounts for 73% of the area covered by rain and 40% of the total rain amount over a 3-yr period (1998–2000). The ratio of the convective rain rate to the stratiform rain rate is 4.1 on average at the horizontal resolution of the PR data. Convective rain rates remain constant or decrease as the stratiform contribution to total rain increases, implying that stratiform rain production is not very dependent on the strength of convection. This relationship is especially evident over the ocean, where there are weaker convective rain rates than over land but relatively larger stratiform rain amounts. The ocean environment appears more efficient in the production of stratiform precipitation through either the sustainability of convection by a warm, moist boundary layer with only a weak diurnal variation and/or by the near–moist adiabatic stratification of the free atmosphere. Factors such as wind shear and the relative humidity of the large-scale environment can also affect the production of stratiform rain.

Over land, higher stratiform rain fractions often occur during the season of maximum insolation and with the occurrence of very large, organized precipitation systems (i.e., mesoscale convective complexes). Monsoon regions show the largest seasonal variations in stratiform rain fraction, with very low values in the season before the monsoon and higher values during the monsoon. A strong gradient in stratiform rain fraction exists across the Pacific, with a minimum ~25% over the Maritime Continent and a maximum ~60% in the intertropical convergence zone (ITCZ) of the eastern-central Pacific. This near-equatorial trans-Pacific gradient becomes exaggerated during El Niño. A higher stratiform rain fraction concentrates latent heating at upper levels, which implies a stronger upper-level circulation response to the heating. Thus, the variations in stratiform rain fraction that occur before the monsoon and during the monsoon, across the Pacific basin, and between La Niña and El Niño imply vertical variations in the large-scale circulation response to tropical precipitating systems that would not occur if the stratiform rain fraction was temporally and spatially uniform across the Tropics.

1. Introduction

A large proportion of tropical precipitation falls from mesoscale cloud systems that develop stratiform precipitation as a result of sheared wind in the environment and/or the natural aging process of convective cells populating the mesoscale cloud systems (Houze 1993, chapter 6; Houze 1997). The net heating profile in the stratiform portions of these cloud systems is distinctly different from that in the convective portions (Houze 1982, 1989). The heating associated with convective rain is positive throughout the profile. The height of maximum heating in the convective regions depends on the size spectrum of the convective elements (Houze et al. 1980; Johnson et al. 1999). The heating profile of stratiform regions is dominated by heating above the 0°C level and cooling below. These profiles combine to produce strong net heating in the mid- to upper troposphere and weak net heating in the lower troposphere. The height of maximum heating and the vertical gradient of the heating profile for the whole precipitating system is largely dependent on the proportion of rain that is convective and stratiform. A higher proportion of stratiform rain concentrates heating at upper levels, which implies a stronger upper-level circulation response. Hartmann et al. (1984) determined that realistically modeling a large-scale tropical response to the heat released by tropical precipitation (i.e., the Walker circulation) required a heating profile based on an ensemble of both convective and stratiform elements, as in an idealized mesoscale convective system. Tao et al. (1993) introduced a method to calculate the three-dimensional latent heating of precipitating clouds across the Tropics based on the amount of rain that is stratiform and convective. Other uses for accurate convective–stratiform partitioning are to validate cumulus parameterizations (Donner et al. 2001), provide data for assimilation in general circulation models (Hou et al. 2001), and further refine area–

* Joint Institute for the Study of the Atmosphere and Ocean Contribution Number 941.

Corresponding author address: Dr. Robert A. Houze, Dept. of Atmospheric Sciences, University of Washington, Box 351640, Seattle, WA 98195-1640.
E-mail: houze@atmos.washington.edu

time integral (ATI) rainfall estimation (Doneaud et al. 1984; Yuter and Houze 1998).

Previous observational studies delineating convective and stratiform precipitation in the Tropics have focused on individual events or locations (e.g., Cheng and Houze 1979; Gamache and Houze 1983; Churchill and Houze 1984; Houze and Rappaport 1984; Leary 1984; Chong and Hauser 1989; Goldenberg et al. 1990; Steiner et al. 1995; Short et al. 1997; Yuter and Houze 1998; Schumacher and Houze 2000; Rickenbach et al. 2002). The variation in the fraction of rain that was stratiform in these studies (25%–85%) implies that the relative importance of convective and stratiform precipitation varies across the Tropics. Up to now there has been no clear indication of the spatial and temporal variations of convective and stratiform precipitation beyond these regional studies carried out for limited time periods.

The coverage of the Tropical Rainfall Measuring Mission (TRMM) Precipitation Radar (PR) allows regional intercomparisons of convective–stratiform contributions to precipitation across the Tropics (20°N–20°S) with data available since the launch of the satellite in November 1997. The PR is perhaps the best available remote-sensing instrument with which to differentiate regions of convective and stratiform precipitation because of its ability to see the three-dimensional structure of the precipitation field at high horizontal and vertical resolution. Reasonable agreement has been found between instantaneous PR convective–stratiform statistics and various airborne and ground-based radar convective–stratiform classifications (Heymsfield et al. 2000; Schumacher and Houze 2000; Liao et al. 2001).

This study presents a 3-yr climatology (1998–2000) of tropical convective–stratiform statistics observed by the TRMM PR, including spatial and temporal variations. The statistics are posed in terms of the amount of rain area classified as stratiform (stratiform rain area fraction), the total rain accounted for by stratiform precipitation (stratiform rain fraction), and the ratio between convective and stratiform rain rates [convective–stratiform (CS) rain-rate ratio]. The emphasis is mostly on stratiform rain fraction because of the direct link between rain and total column latent heating. We focus primarily on patterns observed in the 3-yr climatology that lead to an interpretation of the role of stratiform rain contributions in the general circulation of the Tropics.

2. Data and validation

a. Rain-type classifications

In general, tropical precipitation has two main classifications: convective and stratiform (Houze 1993). Convective precipitation regions are generally identified with intermittently strong vertical velocities ($>|\pm 1$ m $s^{-1}|$), high rain rates (>5 mm h^{-1}), and small ($\sim$1–10-km horizontal dimension), intense, horizontally inhomogeneous radar echo. Stratiform precipitation areas are characterized by statistically small vertical velocities ($<|\pm 1$ m $s^{-1}|$), low rain rates (<5 mm h^{-1}), and widespread ($\sim$100-km horizontal dimension), horizontally homogeneous radar echo. The microphysical processes dominating the growth of particles to precipitation size in convective regions is collection, while the dominant precipitation growth mechanism in stratiform regions is vapor diffusion.

Extensive stratus and stratocumulus cloud decks that have tops well below the 0°C level, and occasionally produce drizzle or light rain, are considered stratiform by standard terminology (Glickman 2000). However, the 17-dB*Z* sensitivity threshold of the TRMM PR guarantees that most, if not all, of this stratiform rain is excluded from this study. The stratiform rain to which this study refers is from deeper cloud systems evolving from or attached to deep convective clouds. In these stratiform clouds, the primary precipitation processes occur in the ice layer above the 0°C level. Fallout and evaporation occur below this level.

Radar reflectivity observations cannot always be unambiguously separated into regions of convective and stratiform precipitation, which occasionally leads to a third ''transition'' or ''intermediary'' classification. However, Mapes and Houze (1995) showed that only two modes account for most of the large-scale atmospheric response to convection and that these modes correspond to the divergence signatures in convective and stratiform precipitation regions. The transition/intermediary region is more closely related to the stratiform region in terms of microphysical and dynamical processes (Houze 1997) such that it remains desirable to separate precipitation into only two categories: that of young, vigorous convection (convective) and that of older, weaker convection (transition/intermediary and stratiform).

b. Precipitation Radar

The PR scans 17° to either side of nadir at intervals of 0.35° with a vertical resolution of 250 m. Until 7 August 2001 the TRMM satellite had an operating altitude of 350 km giving the PR a swath width of 215 km and a horizontal footprint of 4.3 km at nadir. The PR has a precessing orbit so that it may sample the full diurnal cycle. The PR operates at K_u band (2.17-cm wavelength) and is thus subject to strong attenuation. Owing to power constraints, the PR has a relatively low sensitivity of $\sim$17 dB*Z*. However, the PR can detect some reflectivities down to 14 dB*Z* (particularly over the ocean) but not in proportion to actual occurrence. This study uses only data $\geq$17 dB*Z* ($\sim$0.4 mm h^{-1}) to avoid the ambiguity of sampling at lower reflectivities. In addition, the PR is downward-looking but it cannot sense rain directly above the ground because of contamination from the surface return. Thus, this study uses the reflectivity observed closest to the surface that is

free from clutter (normally 1–2 km). Further details on the TRMM satellite and PR can be found in Kummerow et al. (1998) and Kozu et al. (2001). Uncertainties in stratiform rain statistics due to the scanning geometry and sensitivity of the PR are discussed in the appendix.

This study uses a modified version of the PR convective–stratiform rain classifications from version 5 of TRMM product 2A23 (more information available online at http://daac.gsfc.nasa.gov/; Awaka et al. 1997). The PR 2A23 algorithm determines whether the echo is convective or stratiform based on the vertical profile of reflectivity (from which the bright band, echo-top height, and maximum reflectivity in the vertical profile are identified) and the horizontal variability of the echo. The PR convective–stratiform algorithm also assigns echo to a category called ''other'' when there is no bright band detected, the convective reflectivity threshold is not met, and any of the observations below the 0°C level are noise. Thus, the other category either represents noise or regions of precipitation aloft with no precipitation near the surface. Because of the ambiguity of the other category and its very small contribution to total rain ($<0.2\%$ when using the 17-dBZ threshold), this study uses only reflectivity defined as convective or stratiform. It is difficult to validate quantitatively the convective–stratiform echo classification; however, uncertainty is expressed qualitatively in the PR algorithm by assigning to each data point a confidence category based on how strongly the point satisfies the horizontal and vertical criteria. In version 5 of TRMM product 2A23, convective confidence is separated into 10 categories, and stratiform confidence into 6 categories.

In addition, the PR convective–stratiform separation algorithm designates pixels as ''shallow, isolated'' when the echo top is lower than the climatological 0°C level by at least 1.5 km and the pixel is isolated from other rain-certain areas. These shallow, isolated pixels are most prevalent in the light-rain regions of the tropical oceans where very little stratiform rain is expected to occur because of the lack of organized convective systems. Version 5 of TRMM product 2A23 places the majority of the shallow, isolated pixels in a stratiform subcategory; however, the shallow, isolated echoes most likely represent warm rain processes and as such should be classified as convective (Schumacher and Houze 2003). This study reclassifies the stratiform shallow, isolated pixels as convective in order to obtain more reasonable patterns of stratiform rain contribution over the tropical oceans. Version 6 of the algorithm will reflect this reclassification (J. Awaka 2002, personal communication).

This study places the near-surface reflectivity from version 5 of TRMM product 2A25 (Iguchi et al. 2000) into 1-dB bins at 2.5° resolution. The reflectivity is converted into rain rate using version 5 convective and stratiform near-surface initial reflectivity–rain-rate (Z–R) relations of $Z = 148R^{1.55}$ and $Z = 276R^{1.49}$, respectively. In the PR 2A25 algorithm, these Z–R relations are subject to adjustment, based on an attenuation correction and an index of nonuniformity. Since we have changed the convective–stratiform designation of some of the echoes, we must recompute the rain rate at each pixel. For simplicity, we use the initial Z–R relations without adjusting them. The sensitivity of the stratiform rain statistics to variations in Z–R relations is addressed in the appendix. The average convective and stratiform rain rates in each monthly 2.5° grid box are then multiplied by the probability of rain for each rain type to obtain the convective and stratiform rain accumulations.

For most of this study, regions that have less than an equivalent of 0.6 m yr^{-1} of average rain accumulation are not included in order to decrease uncertainty from sampling. Stratiform rain and rain area fraction can become artificially high when the total rain accumulation is too low. The 0.6-m accumulation threshold gives less noisy results in the stratiform rain statistics. This thresholding is further supported by Bell and Kundu (2000) if the relative sampling error for monthly rain amounts is extended to stratiform rain statistics. The stratiform rain statistics are calculated using the histograms of rain information taken in aggregate for the regions and time periods under consideration, that is, stratiform rain statistics are based on total rain volume when considering multiple 2.5° grids.

c. *Kwajalein validation site*

Although Kwajalein represents only one point in the Tropics, it is a useful exercise to validate PR observations for monthly timescales with a continuously operating ground radar. The Kwajalein validation site (8.72°N, 167.73°E) is equipped with an S-band (10 cm), dual-polarization, Doppler weather radar with a beamwidth of 1.12° that collects a three-dimensional volume of data roughly every 10 min. Operationally, the Kwajalein radar (KR) data is interpolated to 2 km in the horizontal and 1.5 km in the vertical. Monthly rain maps are created using all available radar data (if less than 75% of the monthly data is available, no rain map is created). First, the reflectivity values of the Kwajalein radar are calibrated to be consistent with those of the PR by matching the area covered by echo >17 dBZ at 6 km (a height not likely to be affected by attenuation). Second, climatological convective and stratiform reflectivity profiles based on data within 50 km of the KR from over 1300 radar volumes are applied to correct for the height of the lowest beam above the ground. Third, the radar reflectivity data is converted to rain rate using a single climatological Z–R relation, $Z = 175R^{1.5}$. Finally, a gap-filling algorithm is employed to account for missing data. [These steps are further described online at www.atmos.washington.edu/gcg/MG/KWAJ/UW-KWAJrainALG.pdf, and Houze et al. (2003, manuscript submitted to *J. Appl. Meteor.*).]

When comparing monthly observations of the PR and Kwajalein radar, some caveats exist. The Kwajalein ra-

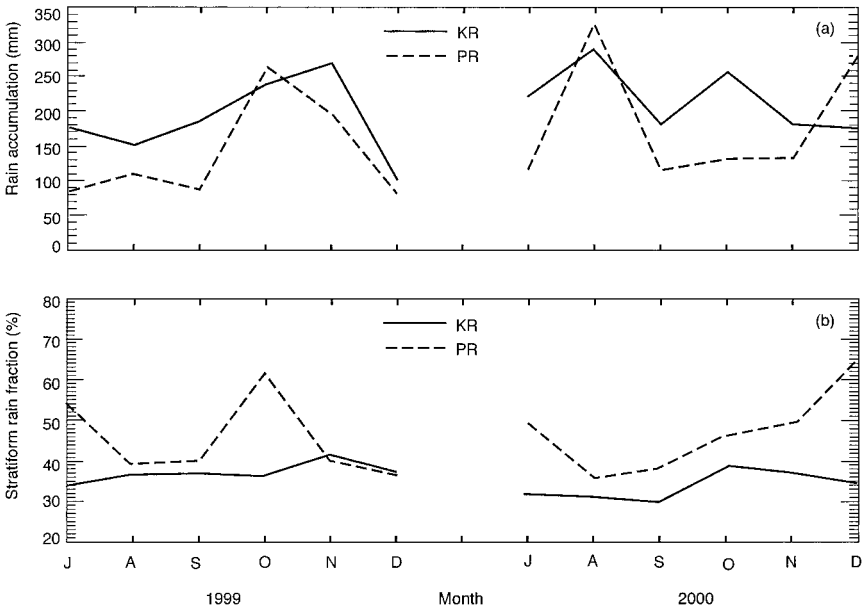

FIG. 1. Kwajalein radar and PR monthly averages within 150 km of the Kwajalein radar from Jun–Dec 1999 and 2000 for (a) rain accumulation and (b) stratiform rain fraction. See text for processing of each dataset.

dar convective–stratiform algorithm utilizes only horizontal information (at 2-km resolution) while the PR convective–stratiform algorithm utilizes both horizontal information (at 4-km resolution) and vertical information (at 250-m resolution). The discrete elevation-angle scans of the ground radar do not provide sufficient vertical resolution to identify the bright band across the whole area covered by the radar. However, bright bands observed close to the radar were used in the tuning of the algorithm (Steiner et al. 1995; Yuter and Houze 1997). The Kwajalein monthly rain and stratiform rain fractions are calculated with near-instantaneous sampling while the PR visits are relatively infrequent. The Kwajalein reflectivities have been corrected to represent surface values whereas the PR reflectivities represent values at the near surface. There is no explicit correction in version 5 of the PR rain profiling algorithm to bring the PR reflectivities to the surface. The Kwajalein rain amounts are based on one local *Z–R* relation applied to both convective and stratiform precipitation, while the PR rain amounts are based on two global relations, one for convective precipitation, the other for stratiform.

Figure 1 compares the average monthly values of rain and stratiform rain fraction as seen by the PR and the Kwajalein ground radar from July to December 1999 and 2000 over the Kwajalein validation site (a 150-km radius around the ground radar or approximately a 2.5° grid). The intermittent sampling of the PR causes the greater month-to-month fluctuations compared to the practically continuous observations by the ground radar. Over the two 6-month periods, the PR observed an average monthly rain accumulation of 161 mm and an average stratiform rain fraction of 46% while the Kwajalein radar showed an average monthly rain accumulation of 203 mm and an average stratiform rain fraction of 34%. Thus, the PR observes less rain and a higher stratiform rain fraction than the Kwajalein radar. A correction to bring PR reflectivities to the surface would increase the PR monthly rain amounts and decrease the stratiform rain fraction, bringing the two radars into better agreement. If the Kwajalein climatological *Z–R* relation is used for the PR data, the PR average rain amounts and stratiform rain fractions both increase. Therefore, the monthly rain amounts of the two radars become even closer but the stratiform rain fraction bias remains, suggesting that the PR may be overclassifying rain as stratiform.

3. Zonal averages

Figure 2 shows the latitude dependence of PR stratiform rain fractions and rain accumulations between 35°N and 35°S for 1998–2000. Zonally averaged stratiform rain fractions are nearly constant at ~40% from 20°N to 20°S and rise rapidly (up to values >50%) in latitudes outside of this equatorial zone (Fig. 2a). The regions outside of 20°N–20°S can receive much of their total rain from midlatitude frontal systems, especially during the local winter. The convective–stratiform algorithm is tuned for the Tropics and may not be applicable to systems subject to extratropical influences.

Zonally averaged rain amounts are low (~0.7 m yr^{-1}) and relatively stable outside of 20°N–20°S while rain amounts are high (up to 1.7 m yr^{-1}) within 20°N–20°S (Fig. 2b). Since the rain accumulations outside of the equatorial region are a factor of 2–3 less than inside of

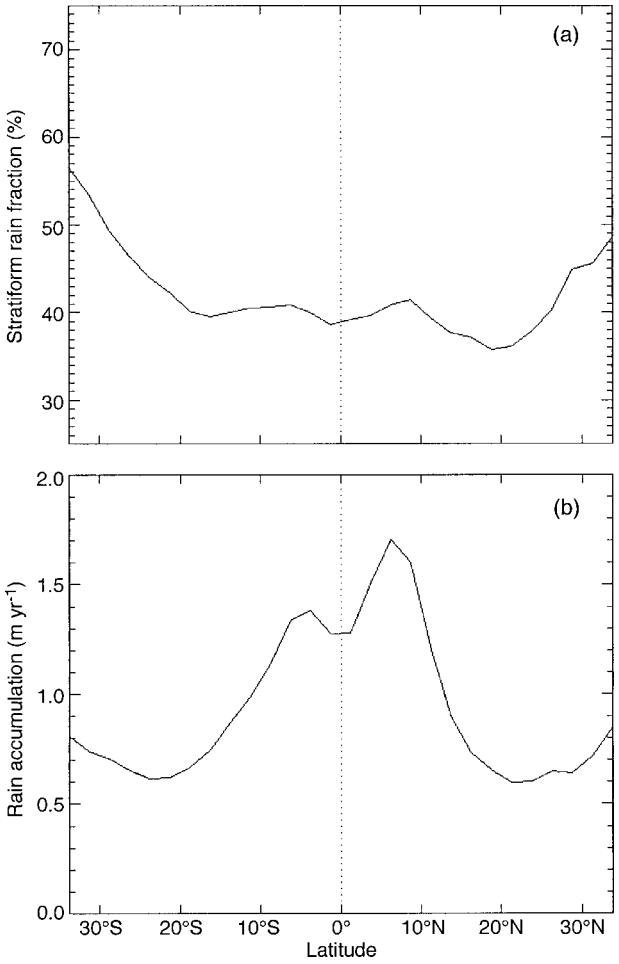

FIG. 2. The PR 2.5° zonal averages at near surface from 1998 to 2000 for (a) stratiform rain fraction and (b) rain accumulation.

the equatorial region, the bulk of the net latent heating occurs from 20°N to 20°S. Because of possible issues of algorithm stability (outside the Tropics and in areas of low rain accumulation) and our desire to concentrate on regions that contribute the most to latent heating, this study will examine stratiform rain statistics between 20°N and 20°S.

4. Annual mean patterns over the Tropics

a. Stratiform rain fraction

As to be expected from the widely varying estimates of tropical stratiform rain fraction previously found in the literature (25%–85%), stratiform rain amount and rain fraction have considerable geographical variability in the PR averages between 20°N and 20°S for 1998–2000. Figures 3b and 3c show the average monthly convective and stratiform rain amounts for the 3-yr period. Convective rain amounts are highest (>1.5 m yr^{-1}) over central Africa, the Maritime Continent, the Amazon into Central America, and the east Atlantic. Stratiform rain amounts tend to be more evenly distributed over land and ocean with values rarely >1.5 m yr^{-1} except over parts of the Maritime Continent and Central America. For reference, Fig. 3a shows the average annual total rain amounts for 1998–2000.

Figure 3d shows the stratiform rain fractions resulting from the above rain distributions. The mean stratiform rain fraction for the 3-yr period is 40% for 20°N–20°S. In general, land regions tend to have lower stratiform rain fractions while oceans have higher fractions. Stratiform rain fractions are lowest (20%–30%) over central Africa, parts of the Maritime Continent, and the Caribbean with other regions $<35\%$ over the Arabian Sea, the Bay of Bengal, eastern Brazil, and the east Atlantic. Stratiform rain fractions are highest (55%–60%) over the intertropical convergence zone (ITCZ) region of the eastern-central Pacific. This maximum is the most prominent feature in the field of stratiform rain fraction. The contrast between this maximum of 55%–60%, over the eastern-central Pacific, and the stratiform rain fractions of 25%–30% over the Maritime Continent have profound implications for the mean east–west circulation over the tropical Pacific (the Walker cell). These differences imply a strong difference in the vertical profile of latent heating between the western and eastern equatorial Pacific. Physical interpretations of the variations in stratiform rain fraction across the Tropics will be discussed further in section 5. In particular section 5c will discuss how the strong west–east gradient of stratiform rain fraction across the Pacific becomes more pronounced during El Niño.

b. Stratiform rain area fraction

Stratiform rain area fraction is defined as the percent of total rain area covered by stratiform rain. While the percent of rain mass that is stratiform indicates the vertical structure of net latent heating by the precipitating clouds, the percent of rain area covered by stratiform rain indicates the vertical structure of the cloud radiative forcing within the precipitating region (Houze 1982, 1989). Geographical variations in stratiform rain area fractions are very similar to variations observed in the stratiform rain fractions and are thus not shown. The relationship between stratiform rain and rain area fractions is discussed in section 4d. The average stratiform rain area fraction between 20°N and 20°S for 1998–2000 is 73%. Therefore, while stratiform precipitation accounts for less than half of the total rain accumulation, it covers the majority of the raining region in the Tropics.

c. Convective–stratiform rain-rate ratio

The CS rain-rate ratio is defined as the mean convective rain rate divided by the mean stratiform rain rate over the 2.5° grid. Rain rates are conditional, that is, based only on areas exhibiting rain. Previous radar stud-

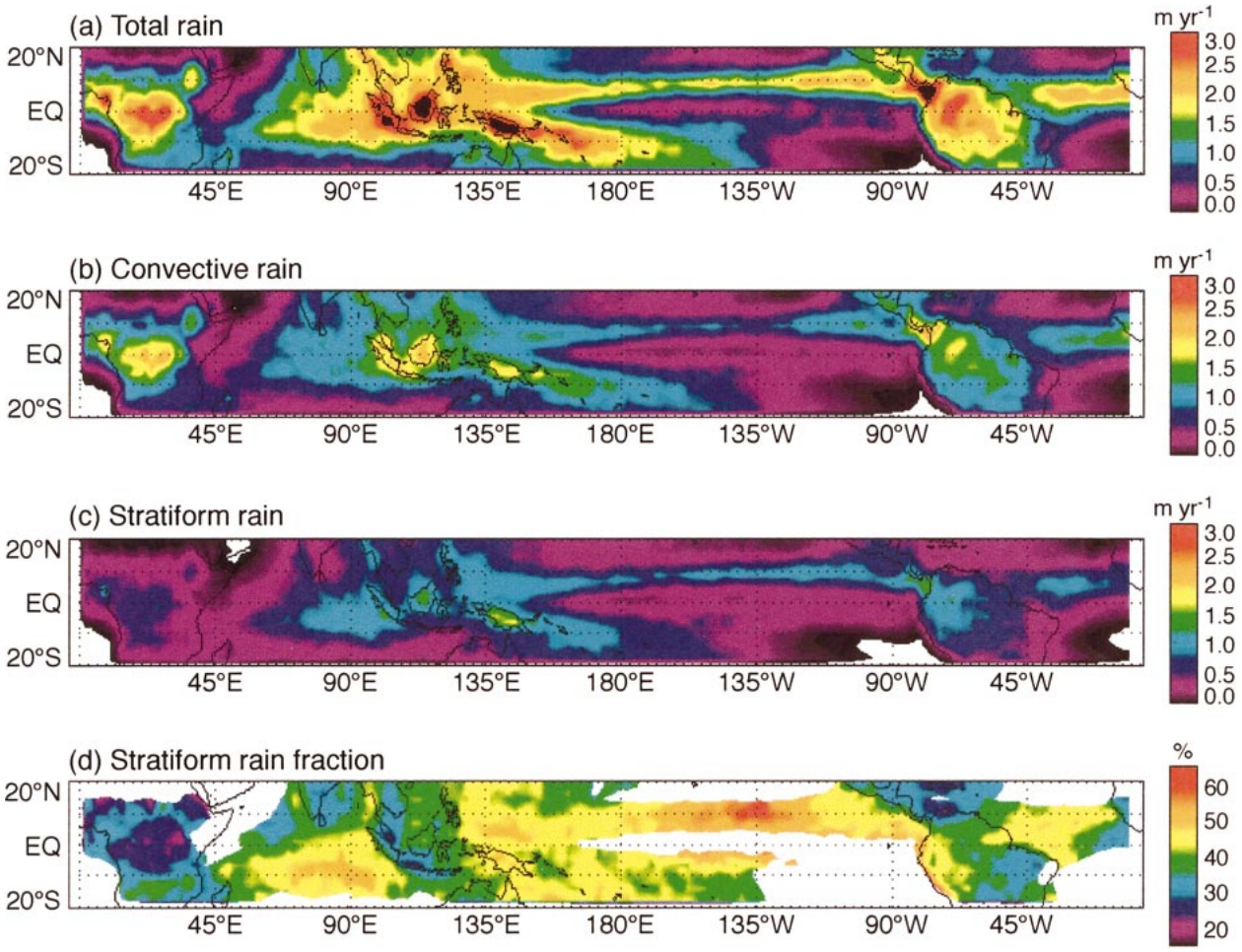

FIG. 3. The PR (a) total rain, (b) convective rain, (c) stratiform rain, and (d) stratiform rain fraction based on a 2.5° grid averages for 1998–2000. Areas with annually averaged rain of less than 0.6 m yr^{-1} were not included in (d).

ies in the Tropics (with horizontal resolutions ranging from 2 to 4 km) have observed that average convective rain rates range from 9 to 14 mm h^{-1} and average stratiform rain rates range from 1 to 4 mm h^{-1} (Gamache and Houze 1983; Leary 1984; Bell and Suhasini 1994; Steiner et al. 1995; Yuter and Houze 1997). The CS rain-rate ratios from the above studies range from 2.6 to 14.

As with the stratiform rain and rain area fractions, there is considerable geographical variability in the PR convective and stratiform rain rates and CS rain-rate ratio averages between 20°N and 20°S for 1998–2000. Convective rain rates range from 3 to 20 mm h^{-1} and are highest ($>$10 mm h^{-1}) over the continents and more moderate (5–7 mm h^{-1}) over the oceans (Fig. 4a). Stratiform rain rates range from 1.2 to 2.7 mm h^{-1}; however, there is little difference between land and ocean (Fig. 4b). The CS rain-rate ratio ranges from 2 to 14 and is $>$5 over most land areas and $<$4 over much of the oceans (Fig. 4c). The overall average convective rain rate observed by the PR is 7.3 mm h^{-1} while the average stratiform rain rate is 1.8 mm h^{-1}. The resulting mean CS rain rate ratio is 4.1.

A notable anomaly from the land-versus-ocean paradigm is the values of about 4 over the Amazon. This region of lower values extends in over the continent from the Atlantic Ocean and is neatly encircled on the west by high CS rain-rate ratios over the Andes. The lower ratios over the Amazon basin are consistent with other studies (Nesbitt et al. 2000; Petersen and Rutledge 2001), which indicate that convection over the Amazon basin is, climatologically, somewhat weaker (or perhaps smaller scale) than typical continental convection. One reason for this fact may be the extension of oceanic environmental characteristics over the land. Garstang et al. (1994) showed the movement of large oceanic mesoscale systems into the Amazon from the Atlantic. The Amazon canopy may also provide the boundary layer some oceanic characteristics (Garstang et al. 1990). Using data collected from a C-band radar located at approximately 10°S, 62.5°W during the TRMM Large-Scale Biosphere Atmosphere (LBA) field campaign,

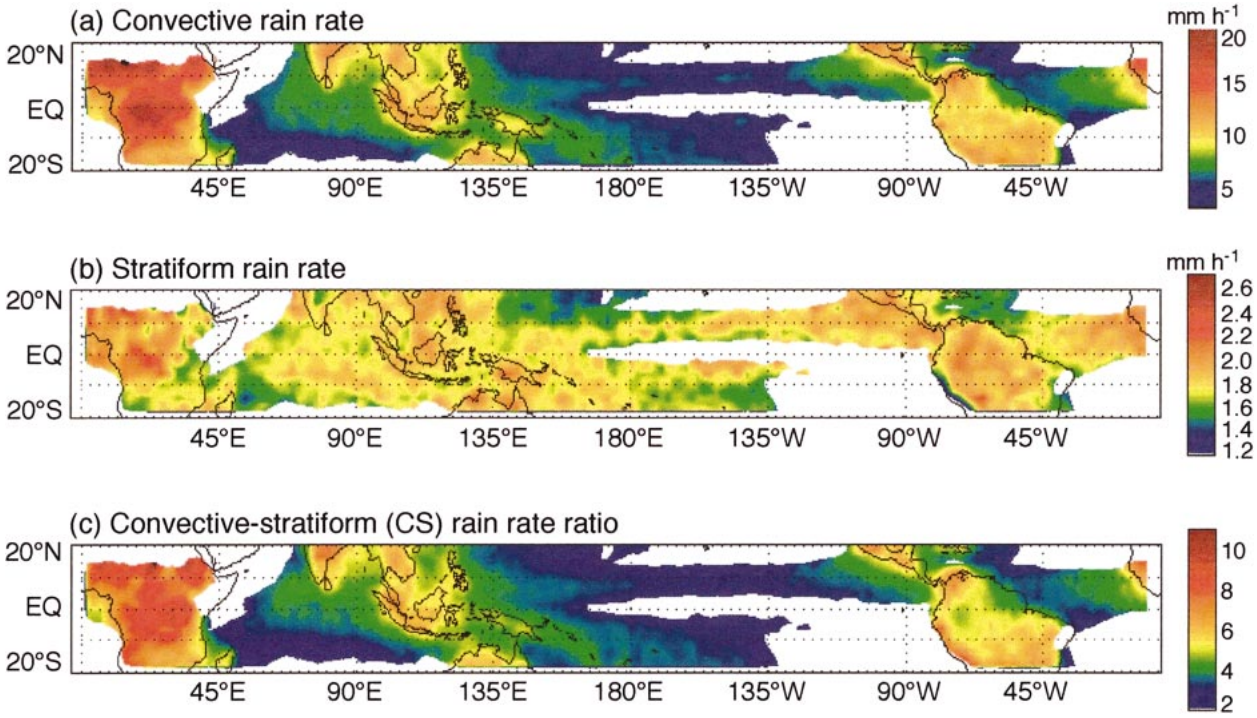

FIG. 4. The PR (a) convective rain rate, (b) stratiform rain rate, and (c) CS rain-rate ratio based on 2.5° grid averages for 1998–2000. Areas with annually averaged rain of less than 0.6 m yr^{-1} were not included.

Rickenbach et al. (2002) showed that convective rain-rates were lower with the presence of the South Atlantic convergence zone (SACZ), while the stratiform rain rates had little regime dependence. Thus the CS rain-rate ratio during LBA decreased dramatically when the stationary fronts that characterize the SACZ were present. This conclusion is consistent with the lower CS rain-rate ratios seen by the PR over the southwestern Amazon in Fig. 4c. More general physical explanations for the convective and stratiform rain-rate variations are addressed in section 5.

d. Relationships among stratiform rain statistics

Figure 5 highlights the range of monthly stratiform rain fractions and explores the relationship of stratiform rain fractions to monthly stratiform rain area fraction, CS rain-rate ratio, and rain. Only 2.5° grids that are between 20°N and 20°S and have rain accumulations greater than 50 mm $month^{-1}$ during 1998–2000 are considered in the two-dimensional histograms.

Monthly stratiform rain fractions range up to 80% while monthly stratiform rain area fractions are rarely less than 40% (Fig. 5a). The correlation between monthly stratiform rain and stratiform rain area fractions is 0.81, which implies that stratiform rain fractions relate closely to the amount of area covered by stratiform rain.

Monthly CS rain-rate ratios range from 2 to 18 (Fig. 5b), similar to the range of CS rain-rate ratios in the literature (2.6–14). The correlation between monthly stratiform rain fraction and CS rain-rate ratio is −0.60, which implies that stratiform rain fractions also relate to the relative rain-rate intensity between convective and stratiform rain. A relatively lower convective rain rate and/or a higher stratiform rain rate are associated with higher stratiform rain fractions. Histograms that show the convective and stratiform rain rates separately versus stratiform rain fraction over land and ocean are shown in Fig. 6 (section 5a).

Figure 5c shows that although the correlation between stratiform rain fraction and monthly rain is low (0.13), there is a tendency for the average monthly stratiform rain fraction to increase with increasing rain amounts; the modal value increases from 35% at 50 mm $month^{-1}$ to 50% at 500 mm $month^{-1}$. Steiner and Houze (1998) found a similar trend in Darwin, Australia, for daily area rainfall. This relationship moreover suggests a tendency for the latent heating in the Tropics to become more concentrated at upper levels as rain amounts increase.

5. Regional climatic regimes

a. Land versus ocean

Studies involving lightning observations clearly indicate a difference in convective intensities between land and ocean with the majority of lightning occurring over land (Jorgensen and LeMone 1989; Lucas et al. 1994; Zipser and Lutz 1994). These studies are corrob-

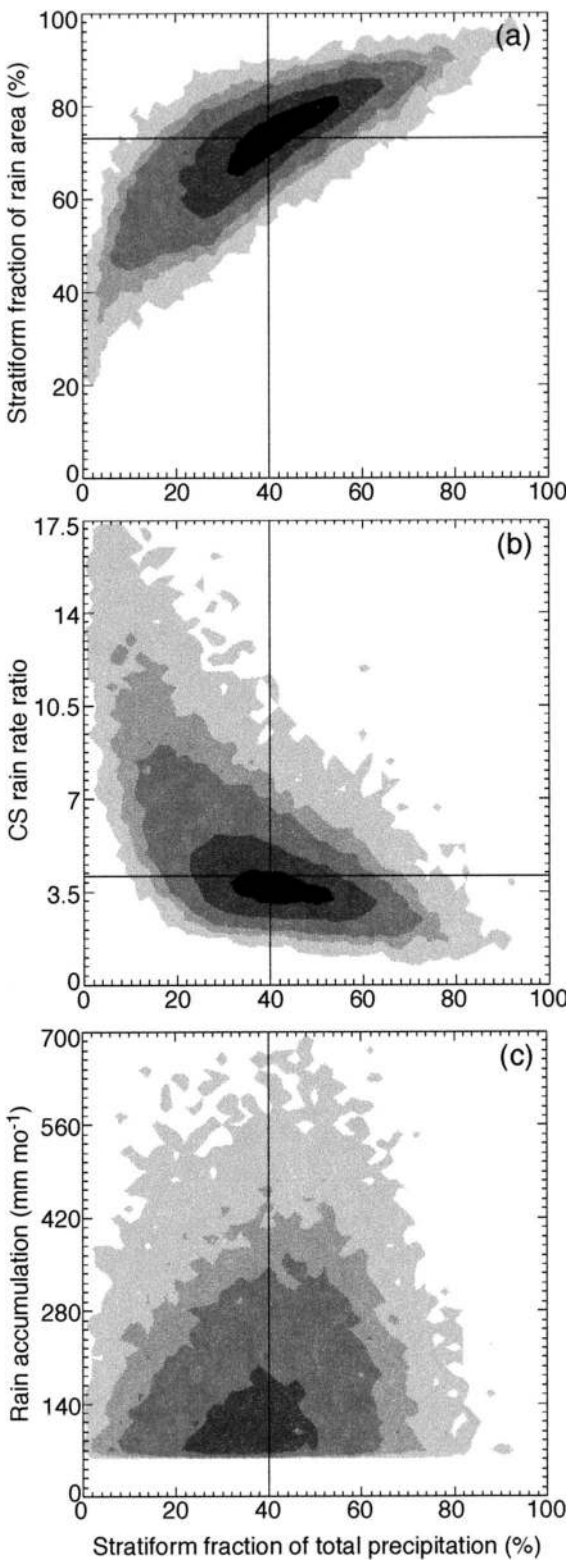

FIG. 5. Two-dimensional histograms of PR monthly stratiform rain fraction vs (a) stratiform area fraction, (b) CS rain-rate ratio, and (c) rain accumulation with bin sizes of 2, 0.35, and 14, respectively. The monthly values are from 1998 to 2000 and represent 2.5° grids within 20°N–20°S. Areas with rain accumulation less than 50 mm month^{-1} were not included. The vertical and horizontal lines indicate the Tropicswide averages. The contours are counts of 1, 10, 25, 100, and 250.

orated by works that have classified other indicators of convective strength over land and ocean, for example, height of the 30-dB*Z* contour, maximum reflectivity at 6 km, and precipitation ice water contents (Nesbitt et al. 2000; Petersen and Rutledge 2001). Also, Steiner et al. (1995) found that near the northern Australian coastline radar-observed land and ocean stratiform rain fractions differed by 13% during the monsoon season.

Table 1 contains bulk percentages of selected quantities for the latitude belt of 20°N–20°S for 1998–2000, split between land and ocean. Stratiform rain accounts for less of the total rain over land (35%) compared to the ocean (43%) but covers slightly more of the total rain area (75% versus 72%). Average convective rain rates are much higher over land (10.2 mm h^{-1}) than ocean (5.8 mm h^{-1}). However, stratiform rain rates are of the same intensity leading to much different land and ocean CS rain-rate ratios (5.5 and 3.3, respectively). The differences between land and ocean stratiform statistics are most likely related to variations in environmental factors, in particular: land versus ocean surface properties, boundary layer thermodynamics, lapse rate in the free atmosphere, and wind shear and relative humidity through the depth of the troposphere. A quantitative investigation of all these factors is beyond the scope of this work. However, some insight may still be gained into the stratiform statistics by qualitative awareness of the general differences in these environmental factors between land and ocean and over different parts of oceans and continents.

When monthly convective rain rates are strong (>10 mm h^{-1}) over land, stratiform rain fractions are negatively correlated with the convective rain intensity (Fig. 6a). One might expect the stronger convection implied by higher convective rain rates to result in larger stratiform rain areas and higher stratiform rain fractions. However, the relationship between the convective rain rate and stratiform rain fraction indicates that the occurrence of significant stratiform precipitation regions is not necessarily indicated by the rain rates of their associated convective cells. Over ocean, average monthly convective rain rates are rarely >10 mm h^{-1} so the stratiform rain fraction appears relatively insensitive to convective rain rates (Fig. 6c). As long as deep convection is present, ocean regions seem proficient at producing stratiform rain, even if the convective rain rates are less than those found over land. Over both land and ocean, stratiform rain rates tend to increase with increasing stratiform rain fraction (Figs. 6b and 6d).

The effective production of stratiform precipitation over the oceans probably results from the near–moist adiabatic stratification of the free atmosphere (Xu and

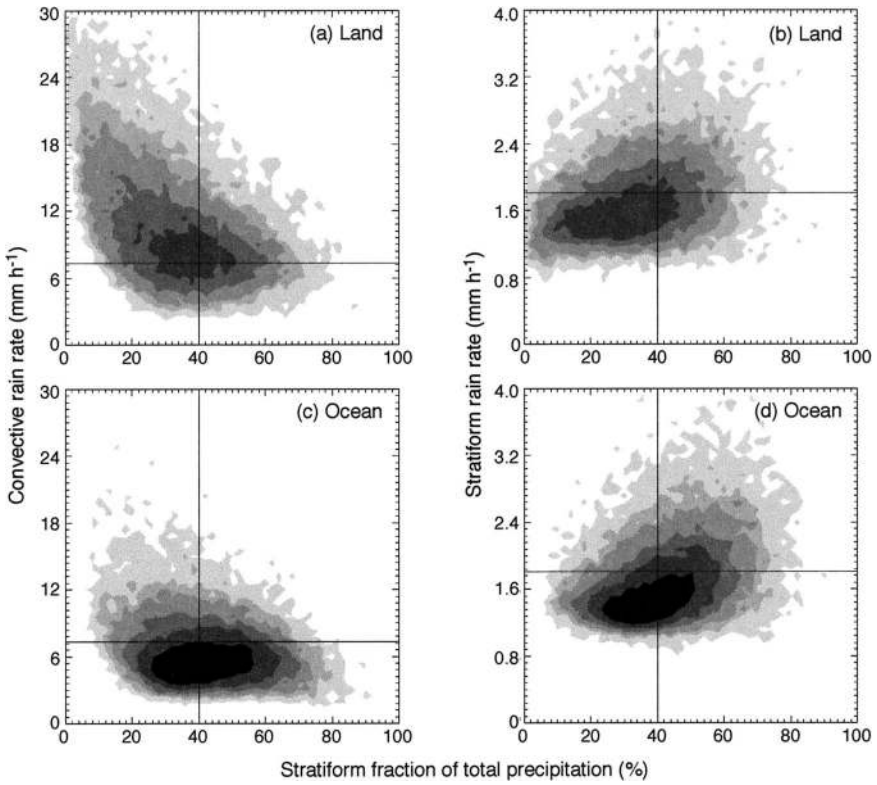

FIG. 6. Two-dimensional histograms of PR monthly stratiform rain fraction vs (a) convective rain rate over land, (b) stratiform rain rate over land, (c) convective rain rate over ocean, and (d) stratiform rain rate over ocean with bin sizes of 0.6 mm h^{-1} for convective rain rates and 0.08 mm h^{-1} for stratiform rain rates. The monthly values are from 1998 to 2000 and represent 2.5° grids within 20°N–20°S. Areas with rain accumulations less than 50 mm $month^{-1}$ were not included. The vertical and horizontal lines indicate the Tropicswide averages. The contours are counts of 1, 5, 10, 25, 50, and 100.

Emanuel 1989) and/or the sustainability of the convection by a warm, moist boundary layer with weak diurnal variation (Yuter and Houze 1998; Kingsmill and Houze 1999). The near–moist adiabatic lapse rates over tropical oceans imply that buoyancy and vertical velocity at lower levels are reduced over ocean compared to over land, where daytime heating creates lower-tropospheric stratification that is closer to dry than moist adiabatic. Nonetheless moderate buoyancy exists at all levels, and convective cells over the ocean often extend to great heights. The generally lower convective rain rates in deep cells over oceans may imply greater generation and transfer of ice hydrometeors aloft into the stratiform regions of oceanic mesoscale convective systems (MCSs). Moreover, the potential for deep convection over the ocean exists through the night, so that it is possible to sustain an MCS for a long time. Because land is subject to a diurnal cycle that shuts down the ability of convective cells to form and stratiform regions to grow, precipitation systems over land do not obtain the stratiform rain fractions observed over the ocean unless some process overcomes the diurnal cycle. In addition, variations in the profiles of relative humidity and wind of the large-scale environment between land and ocean may affect stratiform rain production.

In order to illustrate the above properties, we highlight three regions of different stratiform rain fractions: Africa, the west Pacific warm pool, and the east Pacific ITCZ. Over central Africa (Figs. 3a and 3c, Fig. 4a; 30°E), strong but probably short-lived convection evi-

TABLE 1. Land vs ocean 1998–2000 tropical mean convective and stratiform rain statistics.

	Stratiform rain fraction (%)	Stratiform area fraction (%)	Convective rain rate (mm h^{-1})	Stratiform rain rate (mm h^{-1})	CS rain-rate ratio
All	40	73	7.3	1.8	4.1
Land	35	75	10.2	1.8	5.5
Ocean	43	72	5.8	1.8	3.3

dently produces large rain amounts but relatively little stratiform rain. Two scenarios concerning the microphysics and dynamics of the cloud systems are as follows: 1) the strong (possibly more erect) updrafts related to the large convective rain rates over Africa produce large quantities of water at low levels that rain out and large ice particles at upper levels that fall out, leaving less ice aloft with which to form a robust stratiform region, or 2) the strong (possibly more sheared) updrafts transport more water/ice to upper levels, providing sufficient material to form an extensively raining stratiform region; however, larger-scale environmental factors (such as lower buoyancy aloft or dry air intruding into the developing stratiform region) keep the stratiform precipitation region from attaining its full potential. Over Africa, the dry midlevel Sahara air layer may particularly inhibit the development of moist stratiform regions. The former scenario suggests high convective precipitation efficiency at the expense of the stratiform region; the latter scenario suggests low stratiform precipitation efficiency despite sufficient condensate provided by the convective region. Moreover, the boundary layer shuts down at night, limiting the time available to build a stratiform region. These factors disfavor the development of large, long-lived mesoscale systems with robust stratiform rain regions. Over the west Pacific warm pool (Figs. 3a and 3c, Fig. 4a; 135°E), weaker but probably more frequent convection produces large rain amounts with higher stratiform rain contributions than over Africa. Adapting the above two scenarios to the west Pacific: 1) over the equatorial ocean, the vertical velocities associated with the weaker convective rain rates are more moderate (LeMone and Zipser 1980; Zipser and LeMone 1980) and may extend to high levels to produce smaller ice particles that accumulate in the upper levels and form large stratiform regions, or 2) the more moderate updrafts will transport less water/ice to upper levels but environmental factors, such as a more uniform buoyancy through the depth of the troposphere, less evaporation, and cooperative shear, will allow a large precipitating stratiform region to form. The former scenario suggests a low convective precipitation efficiency that promotes stratiform rain production and the latter scenario suggests a high stratiform precipitation efficiency that overcomes the lessened influx of hydrometeors from the convective region. These processes can continue into and through the night since the boundary layer over the ocean undergoes only slight diurnal variation. The western tropical Pacific is known for large, long-lasting MCSs called superclusters by Nakazawa (1988) and superconvective systems by Chen et al. (1996). Over the eastern-central Pacific (Figs. 3a and 3d, Fig. 4a; 135°W), the total rain is less than over Africa and the west Pacific but the stratiform rain fraction is greatest. The convection is weaker than over Africa (Fig. 4a) and possibly not as sustained as the convection over the west Pacific warm pool. However, the convective cells in the eastern-central Pacific are able to generate sufficient ice to create and maintain stratiform regions that might not seem large compared to the MCSs observed in the west Pacific, but still occur often enough to accumulate fairly large rain amounts.

b. Seasons

1) CONTINENTS

The seasonal stratiform rain fractions range from 20% to 45% over Africa (Fig. 7; 0°–40°E) and from 20% to 50% over Central and South America (Fig. 7; 90°–40°W); the highest fractions occur with the local seasonal solar maximum. Laing and Fritsch (1993a) and Velasco and Fritsch (1987) observed the highest frequency of mesoscale convective complexes (MCCs)[1] at times of seasonal maximum insolation over Africa and Central and South America, respectively. MCCs are often associated with a nocturnal low-level jet constrained by topography. This jet feeds high moist static energy air into the boundary layer, and mesoscale convective systems can grow into the night. This process overcomes the limitation of stratiform rain formation by the diurnal cycle. This result and reasoning suggest that larger stratiform rain fractions over land during the season of maximum solar insolation reflect the frequency of very large, organized precipitation systems (such as MCCs).

Regions that are subject to monsoon circulations also have a distinct seasonal signal in stratiform rain fraction. The Indian subcontinent stratiform rain fractions range from 20% to 45% with sharply lower values during March–April–May (MAM, hereafter all 3-month periods are signified with 3-letter acronyms), the period before the Asian monsoon (Fig. 7b; 70°–85°E). Northern Australia's stratiform fractions range from 25% to 50% with the lowest values during SON, the period before the Australian monsoon (Fig. 7d; 120°–150°E). The increase in stratiform rain fraction during the fully developed monsoon is consistent with the monsoon precipitation forming in maritime air, giving the free atmosphere a more oceanic character. In addition, Laing and Fritsch (1993b) and Miller and Fritsch (1991) found that MCCs occur most frequently when the monsoon extent is greatest in India and Australia, respectively. The fact that increased MCC occurrence coincides with higher stratiform rain fractions during the monsoons again suggests that higher stratiform rain fractions over land could be associated with the occurrence of very large, organized precipitation systems such as MCCs. The increase in both rain and stratiform rain fraction during the fully developed monsoon implies an increase in both the total latent heating and the height of max-

[1] Maddox (1980) defined an MCC as a contiguous area of IR temperature $\leq$221 K with an areal extent $\geq$50 000 km^2 embedded in a contiguous area of IR temperature $\leq$241 K with an areal extent $\geq$100 000 km that lasts 6 h or more and has an eccentricity of $\geq$0.7 at the time of maximum extent.

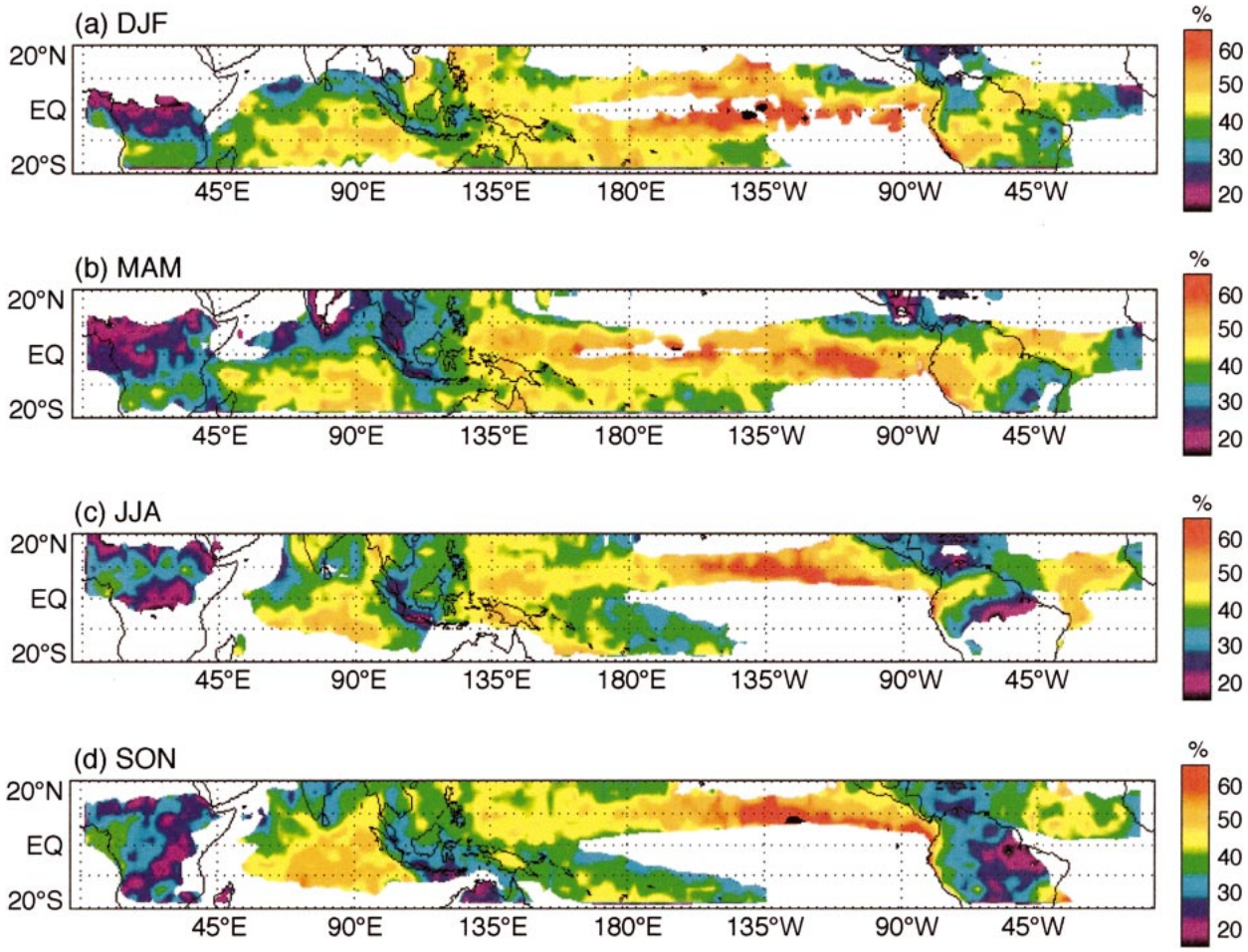

FIG. 7. Seasonal PR stratiform rain fraction based on 2.5° grid averages for 1998–2000. Areas with annually averaged rain of less than 0.6 m yr^{-1} were not included.

imum heating, which leads to an enhanced upper-level circulation response.

The Maritime Continent (Indonesia/Malaysia) has a relatively weak seasonal cycle (Fig. 7; 100°–135°E). The lack of seasonality may be explained by the maritime character of the region. In addition, most of the Maritime Continent does not develop many MCCs (Miller and Fritsch 1991) although large MCSs are frequent (Houze et al. 1981; Williams and Houze 1987).

2) OCEANS

Over most of the tropical oceans, seasonal variations in stratiform rain fraction are smaller than those over land. The west Pacific has the smallest seasonal variability (Fig. 7; 125°–165°E) which may be a result of relatively constant environmental factors, notably sea surface temperature (SST). The east Pacific and east Atlantic have the largest seasonal variability (Fig. 7; 125°–90°W and 25°W–0°). This variability is most likely due to ocean warm-tongue/cold-tongue dynamics (Mitchell and Wallace 1992). The east Pacific and east Atlantic have the highest contribution from stratiform rain in JJA and SON, seasons in which the cold tongue in each ocean basin is most pronounced. The increased cold-tongue/warm-tongue thermal contrast implies an enhanced thermally direct meridional circulation on the scale of the ITCZ. It remains to be shown why this surface-forced circulation should enhance the production of stratiform precipitation by mesoscale cloud systems in the ITCZ region.

Some of the variability in the east Pacific can be linked to the occurrence of the double ITCZ. Often during the boreal spring of non–El Niño years, two bands of convection form and straddle the equator in the east Pacific (Lietzke et al. 2001). The formation of the two bands is caused by a narrow sea surface equatorial cold tongue in a region of low-level wind convergence and otherwise warm SST. The PR observes that there is an asymmetry in stratiform rain fractions between the east Pacific north and south of the equator during March and April of 1999 and 2000 with average stratiform rain fractions of 35% in the northeast and of 50% in the southeast. Rain accumulations were similar for both re-

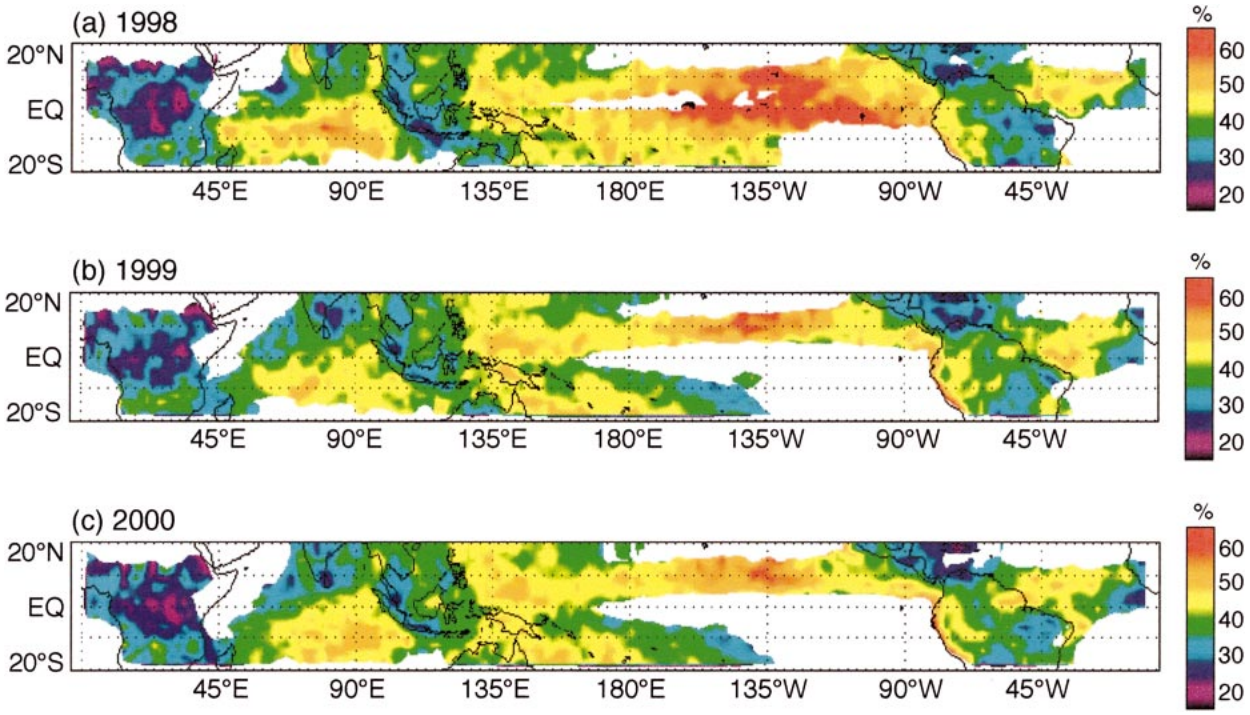

FIG. 8. Annual averages of PR stratiform rain fraction based on 2.5° grid averages for 1998, 1999, and 2000. Areas with annually averaged rain of less than 0.6 m yr^{-1} were not included.

gions. There is little difference in stratiform rain fractions between the two regions in 1998, an El Niño year.

c. Interannual (El Niño–La Niña)

In order to highlight interannual variations in stratiform rain fraction, Figure 8 shows the annually averaged stratiform rain fraction maps for 1998, 1999, and 2000. The largest anomaly occurs in the central and east Pacific (180°–90°W) during 1998, a strong El Niño year. There are no dramatic differences between 1999, a strong La Niña year, and 2000, a normal year. JFMA 1998 and 1999 highlight the longitudinal differences between the El Niño and La Niña events (Fig. 9a). During El Niño, there are lower stratiform rain fractions over the Maritime Continent (20%–30% at 100°–135°E) and higher stratiform rain fractions over the central and east Pacific (50%–60% at 180°–90°W) than during La Niña (~40% for both regions). These signals mirror the well-known rain differences over each region during El Niño, with lower rain amounts over the Maritime Continent and higher rain amounts over the central and east Pacific (Fig. 9b). Similar but smaller oscillations occur over the Indian Ocean (45°–90°E) where stratiform rain fraction and rain amounts increase during El Niño. In this instance, there is a stronger relation between stratiform rain fraction and total rain amount than suggested by Fig. 5c. The fact that an oscillation of stratiform rain fraction accompanies the El Niño–Southern Oscillation of rainfall indicates that *the vertical distribution of heating varies along with the horizontal distribution of heating during these events.* The strong gradient of stratiform rain fraction between the west and east Pacific implies that the maximum of latent heating rises and becomes more concentrated at upper levels in the east and lowers and becomes more vertically elongated in the west during El Niño. This change in heating profile further implies a stronger upper-level atmospheric response to the heating over the eastern-central Pacific during El Niño.

d. Quasi-steady circulations

The land–ocean differences discussed in the previous sections help relate the stratiform rain statistics to specific circulation systems in the Tropics. Webster (1983) highlighted three tropical large-scale structures: the ITCZ, summer monsoons, and semipermanent equatorial convective zones. Figure 10 illustrates regions classified by these large-scale structures. Table 2 ranks the regions from lowest to highest stratiform rain fraction and includes the seasonal stratiform rain fractions for each region.

Overall, the premonsoon regions (West Africa and south Asia during MAM and southern Africa and northern Australia during SON; Table 2 lines 3, 4, 7, 12) tend to have the lowest stratiform rain fractions (19%–33%) followed by the equatorial convective zones (Fig. 10; Table 2 lines 1, 2, 6, 9, 10, 15) with values of 26%–45% and the monsoon regions (West Africa and South

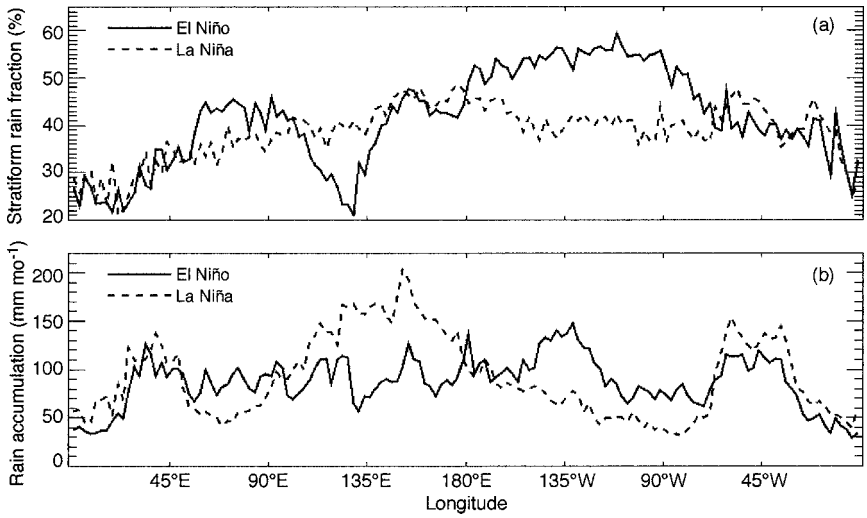

FIG. 9. The PR (a) stratiform rain fraction and (b) rain accumulation longitudinally averaged over 20°N–20°S for Jan–Apr 1998 (El Niño) and Jan–Apr 1999 (La Niña).

Asia during JJA and southern Africa and northern Australia during DJF; Table 2 lines 3, 4, 7, 12) with values of 31%–43%. The ITCZ regions (Fig. 10; Table 2 lines 5, 8, 11, 13, 14, 16–19) have the highest stratiform rain fractions in the Tropics (36%–53%). This breakdown is consistent with Figs. 3d and 7 and the discussion in section 5a in that land environments tend to support less stratiform rain formation than ocean environments. Most likely the premonsoon regions and equatorial convective zones, the majority of which are continental, are subject to intense surface heating and strong diurnal modulation of the boundary layer and therefore have buoyancy concentrated at low levels. The result is intense, shorter-lived convection that is not able to produce significant stratiform regions. The monsoon and ITCZ regions are subject to maritime environments with only weak diurnal modulation and more uniform buoyancy throughout the troposphere that yield weaker but longer-lived convection that can form and maintain significant stratiform regions.

Comparisons of the seasonal stratiform rain fractions in Table 2 indicate that the monsoon regimes have the highest seasonal variability in stratiform rain fractions (>10%), followed by the ITCZ regions (5%–10%), and then the equatorial convective zones (<5%). These seasonal variations are in agreement with Webster's (1983) definitions and descriptions of the large-scale structures. Monsoons are, by nature, itinerant in time and the stratiform rain fractions vary with the seasonal influx of maritime air. Equatorial convective zones, on the other hand, are considered semipermanent and accordingly have more stable stratiform rain fractions. However, some seasonality may be introduced over continental equatorial convective zones by conditions (such as topographically constrained nocturnal low-level jets), which lead to the occurrence of MCCs during the season of maximum solar insolation. ITCZ regions are subject to the meandering of the southeast and northeast trades, which is not great enough to dramatically affect stratiform rain fraction. Exceptions in seasonal variations occur in the ITCZ regions of the east Pacific and east Atlantic (Fig. 10; Table 2 lines 5 and 19), where SST gradients are most pronounced during JJA and SON, and the equatorial convective zone over South America (Fig. 10; Table 2 line 9). These regions have seasonal variations on the order of the monsoons (>10%).

The link between large-scale tropical structures and stratiform rain fraction evident from Table 2 further highlights the role of stratiform rain in dictating the vertical structure of latent heating and thus the response of the circulation to precipitating systems. The fact that the large-scale structures are coherent with stratiform rain fraction suggests that the environments related to these structures play an important role in the evolution of convective precipitation systems that can contribute

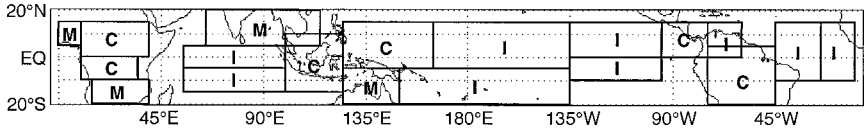

FIG. 10. Quasi-steady circulation regions defined as I (intertropical convergence zone), M (seasonal monsoon regions), and C (semipermanent equatorial convective zones).

TABLE 2. The 1998–2000 stratiform rain fraction rankings for quasi-steady circulation regions. Circulation regions are as defined in Fig. 10. Seasons with rain accumulations less than 50 mm month^{-1} were not included.

	Circulation region	Land/Ocean	Location	ALL	DJF	MAM	JJA	SON
1	C	L	South-central Africa	26	26	28	19	28
2	C	L	North-central Africa	27	—	24	29	29
3	M	L	West Africa	28	—	19*	31**	29
4	M	L	Southern Africa	35	38**	36	—	27*
5	I	O/L	East Atlantic	36	29	32	41	37
6	C	O/L	Maritime Continent	36	39	34	35	35
7	M	L	South and Southeast Asia	36	—	27*	41**	37
8	I	L	Northern South America	36	34	39	38	31
9	C	L	South America	38	43	44	34	28
10	C	L/O	Central America	40	42	37	39	44
11	I	O	North Indian Ocean	41	41	37	41	46
12	M	L/O	Northern Australian	42	43**	45	48	33*
13	I	O	South Pacific	43	46	43	40	39
14	I	O	West Atlantic	43	39	44	47	42
15	C	O	West Pacific warm pool	45	44	47	45	42
16	I	O	South Indian Ocean	47	47	46	47	49
17	I	O	Central Pacific	49	51	48	47	49
18	I	O	Northeast Pacific	49	43	44	52	55
19	I	O	Southeast Pacific	53	—	54	—	—

* Indicates seasons before the monsoon.
** Indicates seasons of the full monsoon.

to the horizontal and vertical gradients of heating that may feedback on large-scale circulation.

6. Conclusions

Using TRMM PR data from across the Tropics (20°N–20°S) for a 3-yr period (1998–2000), we have determined the amount and percentage of rain that is stratiform, the fraction of rain area covered by stratiform precipitation, and the convective and stratiform rain rates along with their ratio. Each of these quantities is useful to large-scale studies of tropical precipitation and atmospheric circulation. The fraction of rain that is stratiform is perhaps most useful because it indicates indirectly the vertical profile of latent heat release (Houze 1982, 1989, 1997). These stratiform rain statistics are dependent both on characteristics of the chosen instrument and on the retrieval algorithm. Thus, the PR rain statistics have a significant range of uncertainty, which is difficult to quantify. The PR is nonetheless a powerful instrument with which to analyze spatial patterns of stratiform rain contribution since it obtains observations from the same, well-calibrated radar using the same convective–stratiform separation and rain profiling algorithms at all locations in the Tropics.

The 3-yr, Tropicswide averages were 40% for stratiform rain fraction, 73% for stratiform rain area fraction, 7.3 mm h^{-1} for convective rain rate, 1.8 mm h^{-1} for stratiform rain rate, and 4.1 for the CS rain-rate ratio. The fraction of rain that is stratiform is positively correlated with the proportion of rain area covered by stratiform rain. Stratiform rain fractions are negatively correlated with the ratio of convective to stratiform rain rates. Convective rain rates remain constant or decrease as the stratiform contribution to total rain increases, implying that stratiform rain production is not very dependent on the strength of convection.

Convective and stratiform rain statistics behave differently over land and ocean. Convective rain rates attain greater values over land, consistent with studies showing that convection over land is stronger on average than over ocean in terms of lightning rates, updraft strength, and reflectivity profiles. Although the ocean has weaker convective rain rates than land, high amounts of rain and large stratiform regions nonetheless occur. The environment over ocean has a more widespread warm, moist boundary layer, which undergoes only a slight diurnal modulation and there is a more uniform buoyancy throughout the troposphere than over land. Thus, the ocean appears as a result to have a more continual formation of convective cells and more effective production of stratiform rain. Factors such as wind shear and relative humidity of the large-scale environment can also affect the production of stratiform rain. Continental regions tend to have smaller stratiform rain fractions than over oceans; however, continental regions have a more pronounced seasonal cycle. Higher values of stratiform rain fraction over land are often associated with the time of seasonal maximum insolation, the occurrence of very large mesoscale systems, and the monsoons.

The fraction of rain that is stratiform is more likely to be larger with higher total rain amounts. This result stresses the importance of stratiform rain in latent heat release and suggests a feedback mechanism with the large-scale circulation. An increase in stratiform rain fraction concentrates the heating at upper levels, implying a stronger upper-level response. If this is coupled

with an increase in rain amount, the upper-level response becomes even stronger, further enhancing the production of stratiform rain. This feedback might be in effect during the monsoons, where the stratiform rain fraction is maximum in the rainy season. A feedback may also occur in the eastern ITCZ regions of the Pacific and Atlantic, where the stratiform rain fraction increases as the SST gradient increases. The stronger upper-level circulation response implied by the increase in stratiform rain fraction may help maintain the meridional circulation (i.e., the cross-equatorial flow) in the ITCZ region. It remains a question why the individual MCSs would produce a higher proportion of stratiform rain when the forcing by the SST gradient is increased.

The most prominent maximum of stratiform rain fraction in the Tropics occurs over the eastern-central Pacific. This maximum is coupled with a pronounced minimum of stratiform rain fraction over the Maritime Continent. This large trans-Pacific gradient of stratiform rain fraction implies a profound difference in the vertical distribution of heating at the eastern and western ends of the near-equatorial Walker cell. This difference becomes exaggerated during El Niño, as the stratiform rain fraction undergoes an interannual oscillation along with the rainfall itself, with the implication that the upper-level circulation strengthens over the eastern-central Pacific during El Niño as a result of the shift of the heating maximum upward.

Raymond (1994) suggested that higher fractions of stratiform rain will tend to strengthen the Hadley and Walker circulations. Our results are consistent with his suggestion. As noted above, the relationship is also evident during the monsoons. The TRMM PR data collected for 3 yr thus indicate the Tropicswide patterns in which stratiform rain fraction increases in concert with rainfall and/or SST gradient in such a way as to enhance the Hadley, Walker, and monsoonal circulations.

We have two follow-up studies in progress to pursue the broader implications of this feedback and to understand it better. In the first of these studies, we are examining the global circulation response of a climate model to the spatially varying heating implied by the TRMM-observed fields of rainfall and stratiform rain fraction. In the second study we are conducting a joint analysis of global numerical model reanalysis fields and the temporal and geographic variations of stratiform rain fraction to relate the TRMM PR stratiform rain statistics to environmental variables such as wind shear, SST, and relative humidity.

Acknowledgments. We thank Alan Betts for comments that helped refine this paper. Candace Gudmundson edited the paper and Kay Dewar and Jill Campbell refined the figures. This research was supported by the following grants: NASA #NGT5-30378, NASA #NAG5-9668, NSF #ATM-9900710, NASA #NAG5-4795, and the University of Washington Joint Institute for the Study of the Atmosphere and Ocean (JISAO) Cooperative Agreement #NA67R50155 (JASMINE, GCIP, and PACS).

APPENDIX

Retrieval Uncertainties in the PR Convective and Stratiform Rain Statistics

a. Scanning geometry and wavelength of the PR

The quasi-vertically pointing PR has relatively good vertical resolution (250 m at nadir) with which to define the bright band, a good indicator of stratiform rain. However, bright band detection is beam-angle dependent and can be as low as 20% at the antenna scan edge (TRMM PR algorithm instruction manual, version 1). The PR's horizontal resolution is >4 km, which is marginal for defining individual convective cells (normally on the order of 1–2 km). The PR's horizontal resolution became ~ 5 km after the increase in operating altitude in August 2001, exacerbating this problem. The PR operates at an attenuating wavelength (K_u band), which significantly reduces the apparent intensity of convective cells near the surface. The PR's convective–stratiform separation (Awaka et al. 1997) is applied to reflectivity data that are not corrected for attenuation. Therefore, the PR's low horizontal resolution and attenuation may lead the algorithm to alias some convective echoes into the stratiform category.

b. Changes of reflectivity with height

The convective–stratiform proportions may change below the 0°C level and the surface because of the differential change of reflectivity with height in convective and stratiform profiles (Zipser and Lutz 1994; DeMott and Rutledge 1998; Steiner and Houze 1998). Over land and ocean, stratiform reflectivity profiles tend to be constant with height below the 0°C level. Over the tropical oceans, convective reflectivities increase toward the surface while over land in the Tropics, the maximum in the convective profile is somewhere between the surface and the 0°C level. The horizontal method in the PR convective–stratiform algorithm uses the lowest level that is free from surface clutter (ranging from 1 at nadir to 2 km at the antenna scan edge). Thus, over the ocean, one would expect the stratiform rain fraction to decrease and the CS rain-rate ratio to increase toward the surface while the opposite trend would occur over land.

c. PR sensitivity

The PR has limited sensitivity to very light precipitation ($\sim$17 dBZ). While it can capture all but $\sim$3% of surface rain amount, it can miss up to 50% of the rain area greater than 0 dBZ observed by a ground radar (Schumacher and Houze 2000). In addition, the low sensitivity of the PR affects the convective and strati-

TABLE A1. The 1998–2000 tropical mean convective and stratiform rain statistic sensitivities to the PR reflectivity threshold.

Reflectivity threshold (dBZ)	Stratiform rain fraction (%)	Stratiform area fraction (%)	Convective rain rate (mm h^{-1})	Stratiform rain rate (mm h^{-1})	CS rain-rate ratio
18	40	72	7.4	1.9	4.0
20	39	71	7.7	2.0	3.8
22	38	69	8.3	2.3	3.6

TABLE A2. The 1998–2000 tropical mean convective and stratiform rain statistic sensitivities to the exponent, *b*, in the *Z–R* relation.

b	Stratiform rain fraction (%)	Convective rain rate (mm h^{-1})	Stratiform rain rate (mm h^{-1})	CS rain-rate ratio
PR initial	40	7.3	1.8	4.1
1.3	42	7.1	1.9	3.7
1.4	45	5.8	1.8	3.3
1.5	48	5.0	1.7	3.0
1.6	50	4.3	1.6	2.7

form rain rates (especially compared to what a rain gauge or ground radar might measure) thus affecting the CS rain-rate ratio. Table A1 shows the trend that a decreasing PR sensitivity would have on tropical mean stratiform rain statistics. Assuming a 22-dBZ reflectivity threshold, stratiform rain fraction decreases to 38%, stratiform rain area fraction decreases to 69%, convective rain rate increases to 8.3 mm h^{-1}, stratiform rain rate increases to 2.3 mm h^{-1} and the CS rain-rate ratio decreases to 3.6. An opposite trend should occur with increasing sensitivity but cannot be determined quantitatively with PR data.

The limited sensitivity of the PR, on the other hand, can contribute to an increase of the stratiform component. To identify convective cells, the horizontal method of the PR's convective–stratiform separation algorithm needs to compare a convective core reflectivity to a background rate. If the background rate falls below the threshold of sensitivity, the algorithm has no way to determine if an observed small patch of echo is convective or not. In these cases the echo is considered stratiform. In attempts to account for this effect, the shallow, isolated cells identified as stratiform by the PR algorithm were placed in the convective category to obtain a more realistic pattern of stratiform rain contributions (Schumacher and Houze 2003).

d. Z–R relation

In a study of the Darwin, Australia, coastal radar, Steiner and Houze (1997) found that the uncertainty in the ground radar's monthly stratiform rain fraction due only to the choice of *Z–R* relation is about ±20%. Half of this uncertainty is from the choice of the exponent, *b*, while the other half is from the choice of whether to use a single or multiple *Z–R* relations. Work by Ciach et al. (1997) and Yuter and Houze (1997) suggests that for radar echoes over the tropical ocean there is no statistical justification for applying separate convective and stratiform *Z–R* relations when convective and stratiform rain areas are distinguished solely by typical radar observations. The choice of *b* is therefore more relevant to this discussion. Table A2 shows that the range of the mean tropical stratiform rain fraction is 42%–50% when the exponent, *b*, in a single *Z–R* relation ($300R^b$) is varied between 1.3 and 1.6. These *b* values represent expected climatological values (Doelling et al. 1998; Steiner and Smith 2000). Similarly, the mean convective rain rate ranges from 7.1 to 4.3 mm h^{-1}, the mean stratiform rain rate ranges from 1.9 to 1.6 mm h^{-1}, and the CS rain-rate ratio ranges from 3.7 to 2.7 when the *b* is varied between 1.3 and 1.6. Stratiform rain area fractions are not affected by the choice of the *Z–R* relation. The PR uses separate convective and stratiform *Z–R* relations but its estimate of mean stratiform rain fraction is similar to the single *Z–R* relation means when $b = 1.3$. This study uses the initial *Z–R* relations from the PR algorithm because the resulting stratiform rain statistics are similar to what is available to the general community; however, there is as yet no definitive evidence supporting the use of a single or double *Z–R* relation for rain-rate estimation.

REFERENCES

Awaka, J., T. Iguchi, H. Kumagai, and K. Okamoto, 1997: Rain type classification algorithm for TRMM precipitation radar. *Proc. 1997 Int. Geoscience and Remote Sensing Symp.*, Singapore, IEEE, 1633–1635.

Bell, T. L., and R. Suhasini, 1994: Principal modes of variation of rain-rate probability distributions. *J. Appl. Meteor.*, **33,** 1067–1078.

——, and P. K. Kundu, 2000: Dependence of satellite sampling error on monthly averaged rain rates: Comparison of simple models and recent studies. *J. Climate,* **13,** 449–462.

Chen, S. S., R. A. Houze Jr., and B. E. Mapes, 1996: Multiscale variability of deep convection in relation to large-scale circulation in TOGA COARE. *J. Atmos. Sci.*, **53,** 1380–1409.

Cheng, C., and R. A. Houze Jr., 1979: The distribution of convective and mesoscale precipitation in GATE radar echo patterns. *Mon. Wea. Rev.*, **107,** 1370–1381.

Chong, M., and D. Hauser, 1989: A tropical squall line observed during the COPT 81 Experiment in West Africa. Part II: Water budget. *Mon. Wea. Rev.,* **117,** 728–744.

Churchill, D. D., and R. A. Houze Jr., 1984: Development and structure of winter monsoon cloud clusters on 10 December 1978. *J. Atmos. Sci.,* **41,** 933–960.

Ciach, G. J., W. F. Krajewski, E. N. Anagnostou, M. L. Baeck, J. A. Smith, J. R. McCollum, and A. Kruger, 1997: Radar rainfall estimation for ground validation studies of the Tropical Rainfall Measuring Mission. *J. Appl. Meteor.,* **36,** 735–747.

DeMott, C. A., and S. A. Rutledge, 1998: The vertical structure of TOGA COARE convection. Part II: Modulating influences and implications for diabatic heating. *J. Atmos. Sci.*, **55,** 2748–2762.

Doelling, I. G., J. Joss, and J. Riedl, 1998: Systematic variations of *Z–R* relationships from drop size distributions measured in northern Germany during seven years. *Atmos. Res.,* **47–48,** 635–649.

Doneaud, A. A., S. Ionescu-Niscov, D. L. Priegnitz, and P. L. Smith, 1984: The Area–Time Integral as an indicator for convective rain volumes. *J. Climate Appl. Meteor.,* **23,** 555–561.

Donner, L. J., C. J. Seman, and R. S. Hemler, 2001: A cumulus parameterization including mass fluxes, convective vertical velocities, and mesoscale effects: Thermodynamic and hydrological aspects in a general circulation model. *J. Climate,* **14,** 3444–3463.

Gamache, J. F., and R. A. Houze Jr., 1983: Water budget of a mesoscale convective system in the tropics. *J. Atmos. Sci.,* **40,** 1835–1850.

Garstang, M., and Coauthors, 1990: The Amazon Boundary-Layer Experiment (ABLE 2B): A meteorological perspective. *Bull. Amer. Meteor. Soc.,* **71,** 19–32.

——, H. L. Massie Jr., J. Halverson, S. Greco, and J. Scala, 1994: Amazon coastal squall lines. Part I: Structure and kinematics. *Mon. Wea. Rev.,* **122,** 608–622.

Glickman, T. S., Ed., 2000: *Glossary of Meteorology*. 2d ed. Amer. Meteor. Soc., 855 pp.

Goldenberg, S. B., R. A. Houze Jr., and D. D. Churchill, 1990: Convective and stratiform components of a winter monsoon cloud cluster determined from geosynchronous IR satellite data. *J. Meteor. Soc. Japan,* **68,** 37–63.

Hartmann, D. L., H. H. Hendon, and R. A. Houze Jr., 1984: Some implications of the mesoscale circulations in tropical cloud clusters for large-scale dynamics and climate. *J. Atmos. Sci.,* **41,** 113–121.

Heymsfield, G., B. Geerts, and L. Tian, 2000: TRMM Precipitation Radar reflectivity profiles as compared with high-resolution airborne and ground-based radar measurements. *J. Appl. Meteor.,* **39,** 2080–2102.

Hou, A. Y., S. Q. Zhang, A. M. da Silva, W. S. Olson, C. D. Kummerow, and J. Simpson, 2001: Improving global analysis and short-range forecast using rainfall and moisture observations derived from TRMM and SSM/I passive microwave sensors. *Bull. Amer. Meteor. Soc.,* **82,** 659–679.

Houze, R. A., Jr., 1982: Cloud clusters and large-scale vertical motions in the tropics. *J. Meteor. Soc. Japan,* **60,** 396–410.

——, 1989: Observed structure of mesoscale convective systems and implications for large-scale heating. *Quart. J. Roy. Meteor. Soc.,* **115,** 425–461.

——, 1993: *Cloud Dynamics*. Academic Press, 573 pp.

——, 1997: Stratiform precipitation in regions of convection: A meteorological paradox? *Bull. Amer. Meteor. Soc.,* **78,** 2179–2196.

——, and E. N. Rappaport, 1984: Air motions and precipitation structure of an early summer squall line over the eastern tropical Atlantic. *J. Atmos. Sci.,* **41,** 553–574.

——, C. P. Cheng, C. A. Leary, and J. F. Gamache, 1980: Diagnosis of cloud mass and heat fluxes from radar and synoptic data. *J. Atmos. Sci.,* **37,** 754–773.

——, S. G. Geotis, F. D. Marks Jr., and A. K. West, 1981: Winter monsoon convection in the vicinity of North Borneo. Part I: Structure and time variation of the clouds and precipitation. *Mon. Wea. Rev.,* **109,** 1595–1614.

Iguchi, T., T. Kozu, R. Meneghini, J. Awaka, and K. Okamoto, 2000: Rain-profiling algorithm for the TRMM Precipitation Radar. *J. Appl. Meteor.,* **39,** 2038–2052.

Johnson, R. H., T. M. Rickenbach, S. A. Rutledge, P. E. Ciesielski, and W. H. Schubert, 1999: Trimodal characteristics of tropical convection. *J. Climate,* **12,** 2397–2418.

Jorgensen, D. P., and M. A. LeMone, 1989: Vertical velocity characteristics of oceanic convection. *J. Atmos. Sci.,* **46,** 621–640.

Kingsmill, D. E., and R. A. Houze Jr., 1999: Thermodynamic characteristics of air flowing into and out of precipitating convection over the west Pacific warm pool. *Quart. J. Roy. Meteor. Soc.,* **125,** 1209–1229.

Kozu, T., and Coauthors, 2001: Development of precipitation radar onboard the Tropical Rainfall Measuring Mission (TRMM) satellite. *IEEE Trans. Geosci. Remote Sens.,* **39,** 102–116.

Kummerow, C., W. Barnes, T. Kozu, J. Shiue, and J. Simpson, 1998: The Tropical Rainfall Measuring Mission (TRMM) sensor package. *J. Atmos. Oceanic Technol.,* **15,** 809–817.

Laing, A. G., and J. M. Fritsch, 1993a: Mesoscale convective complexes in Africa. *Mon. Wea. Rev.,* **121,** 2254–2263.

——, and ——, 1993b: Mesoscale convective complexes over the Indian monsoon region. *J. Climate,* **6,** 911–919.

Leary, C. A., 1984: Precipitation structure of the cloud clusters in a tropical easterly wave. *Mon. Wea. Rev.,* **112,** 313–325.

LeMone, M. A., and E. J. Zipser, 1980: Cumulonimbus vertical velocity events in GATE. Part I: Diameter, intensity and mass flux. *J. Atmos. Sci.,* **37,** 2444–2457.

Liao, L., R. Meneghini, and T. Iguchi, 2001: Comparisons of rain rate and reflectivity factor derived from the TRMM Precipitation Radar and the WSR-88D over the Melbourne, Florida site. *J. Atmos. Oceanic Technol.,* **18,** 1959–1974.

Lietzke, C. E., C. Deser, and T. H. Vonder Haar, 2001: Evolutionary structure of the eastern Pacific double ITCZ based on satellite moisture profile retrievals. *J. Climate,* **14,** 743–751.

Lucas, C., E. J. Zipser, and M. A. LeMone, 1994: Vertical velocity in oceanic convection. *J. Atmos. Sci.,* **51,** 3183–3193.

Maddox, R. A., 1980: Mesoscale convective complexes. *Bull. Amer. Meteor. Soc.,* **61,** 1374–1387.

Mapes, B. E., and R. A. Houze Jr., 1995: Diabatic divergence profiles in western Pacific mesoscale convective systems. *J. Atmos. Sci.,* **52,** 1807–1828.

Miller, D., and J. M. Fritsch, 1991: Mesoscale convective complexes in the western Pacific region. *Mon. Wea. Rev.,* **119,** 2978–2990.

Mitchell, T. P., and J. M. Wallace, 1992: The annual cycle in equatorial convection and sea surface temperature. *J. Climate,* **5,** 1140–1156.

Nakazawa, T., 1988: Tropical super clusters within intraseasonal variations over the western Pacific. *J. Meteor. Soc. Japan,* **66,** 823–839.

Nesbitt, S. W., E. J. Zipser, and D. J. Cecil, 2000: A census of precipitation features in the Tropics using TRMM: Radar, ice scattering, and ice observations. *J. Climate,* **13,** 4087–4106.

Petersen, W. A., and S. A. Rutledge, 2001: Regional variability in tropical convection: Observations from TRMM. *J. Climate,* **14,** 3566–3586.

Raymond, D. J., 1994: Convective processes and tropical atmospheric circulations. *Quart. J. Roy. Meteor. Soc.,* **120,** 1431–1455.

Rickenbach, T. M., R. N. Ferreira, J. B. Halverson, D. L. Herdies, and M. A. F. Silva Dias, 2002: Modulation of convection in the southwestern Amazon basin by extratropical stationary fronts. *J. Geophys. Res.,* **107** (D20), 8040, doi:10.1029/2000JD000263.

Schumacher, C., and R. A. Houze Jr., 2000: Comparison of radar data from the TRMM satellite and Kwajalein oceanic validation site. *J. Appl. Meteor.,* **39,** 2151–2164.

——, and ——, 2003: The TRMM Precipitation Radar's view of shallow, isolated rain. *J. Appl. Meteor.,* in press.

Short, D. A., P. A. Kucera, B. S. Ferrier, J. C. Gerlach, S. A. Rutledge, and O. W. Thiele, 1997: Shipboard radar rainfall patterns within the TOGA COARE IFA. *Bull. Amer. Meteor. Soc.,* **78,** 2817–2836.

Steiner, M., and R. A. Houze Jr., 1997: Sensitivity of the estimated monthly convective rain fraction to the choice of *Z–R* relation. *J. Appl. Meteor.,* **36,** 452–462.

——, and ——, 1998: Sensitivity of monthly three-dimensional radar-echo characteristics to sampling frequency. *J. Meteor. Soc. Japan,* **76,** 73–95.

——, and J. A. Smith, 2000: Reflectivity, rain rate, and kinetic energy flux relationships based on raindrop spectra. *J. Appl. Meteor.,* **39,** 1923–1940.

——, R. A. Houze Jr., and S. E. Yuter, 1995: Climatological characterization of three-dimensional storm structure from operational radar and rain gauge data. *J. Appl. Meteor.,* **34,** 1978–2007.

Tao, W. K., S. Lang, J. Simpson, and R. Adler, 1993: Retrieval algorithms for estimating the vertical profiles of latent heat release: Their applications for TRMM. *J. Meteor. Soc. Japan,* **71,** 685–700.

Velasco, I., and J. M. Fritsch, 1987: Mesoscale convective complexes in the Americas. *J. Geophys. Res.,* **92,** 9591–9613.

Webster, P. J., 1983: Large-scale structure of the tropical atmosphere. *Large-Scale Dynamical Processes in the Atmosphere,* B. J. Hoskins and R. F. Pearce, Eds., Academic Press, 235–275.

Williams, M., and R. A. Houze Jr., 1987: Satellite-observed characteristics of winter monsoon cloud clusters. *Mon. Wea. Rev.,* **115,** 505–519.

Xu, K., and K. A. Emanuel, 1989: Is the tropical atmosphere conditionally unstable? *Mon. Wea. Rev.,* **117,** 1471–1479.

Yuter, S. E., and R. A. Houze Jr., 1997: Measurements of raindrop size distribution over the Pacific warm pool and implications for *Z–R* relations. *J. Appl. Meteor.,* **36,** 847–867.

——, and ——, 1998: The natural variability of precipitating clouds over the western Pacific warm pool. *Quart. J. Roy. Meteor. Soc.,* **124,** 53–99.

Zipser, E. J., and M. A. LeMone, 1980: Cumulonimbus vertical velocity events in GATE. Part II: Synthesis and model core structure. *J. Atmos. Sci.,* **37,** 2458–2469.

——, and K. R. Lutz, 1994: The vertical profile of radar reflectivity of convective cells: A strong indicator of storm intensity and lightning probability? *Mon. Wea. Rev.,* **122,** 1751–1759.